SAND2024-14113R
LDRD PROJECT NUMBER: 233049
LDRD PROJECT TITLE: Ultrafast Surface Phosphor Thermometry for Pulsed-power and Hostile Environments
PROJECT TEAM MEMBERS: Caroline Winters, Noelle Collins, Joseph Klesko, Luke McClintock, Tenzin Norden, Shannon Murray, Seth Davis, Nichole Valdez, Ryan Khan, Sadhvikas Addamane, Alex Sarracino.

ABSTRACT:

Modern concepts for next generation pulsed power (NGPP) are slated to deliver up to ten times the energy of Z today. An increase of this magnitude is concerning insofar that Z currently exhibits sizable amounts of inner magnetically insulated transmission line (MITL) loss current on the order of 5-10% [1]. Loss phenomenon in these systems are complex and electrode heating and subsequent thermal desorption are a leading cause [2]. Rapid heat-driven thermal desorption of contaminants scales as the square of the current [1,3,4]. Therefore, even a modest doubling of drive current would yield an ~ 4X in non-linear surface electrode heating, quickening thermal desorption-based current loss. Exacerbating these physics is a current inability to measure ultra-fast heating rates (>20°C/ns), which are paramount to benchmarking and code validation critical to NGPP design – as an empirical approach is not viable.

Therefore, Ultrafast Photoluminescent Surface Heating Optical Thermometry (UP-SHOT) was developed as a new diagnostic for measurement of GHz-scale electrode heating. The discovery of UP-SHOT leveraged expertise in Engineering Science, Material Science, Pulsed-Power, and the Center for Integrated Nanotechnologies.

This report includes information on:
1) The preparation of zinc oxide (ZnO) films, characterization, post-deposition treatments
2) Time-resolved photoluminescence at elevated temperatures and thermographic sensitivity

INTRODUCTION AND EXECUTIVE SUMMARY OF RESULTS:

In high-energy density physics (HEDP) experiments, accurately gauging incident power poses a significant challenge, crucial for understanding these extreme environments and their loss mechanisms [5,6]. Traditional power measurement techniques falter under the extreme conditions of HEDP experiments and the rapid dynamics involved, leaving critical loss mechanisms like chemical desorption poorly understood [1,7]. Consequently, there's a pressing need for non-invasive, in situ temperature measurements, which offer a good representation of power flow in these experiments. Current methods, however, struggle to combine the necessary rapid response times with the durability required for these conditions. To address this gap, we present the UP-SHOT technique, utilizing Zinc Oxide (ZnO) thin films for rapid and precise temperature measurements. This novel approach not only promises to overcome the limitations of existing

Sandia National Laboratories is a multimission laboratory managed and operated by National Technology and Engineering Solutions of Sandia, LLC, a wholly owned subsidiary of Honeywell International, Inc., for the U.S. Department of Energy's National Nuclear Security Administration under contract DE-NA-0003525.

methods but also provides new insights into the fundamental thermal behavior of ZnO thin films at elevated temperatures.

Current thermometry techniques fail to meet the rigorous requirements of HEDP experiments, due to their inability to simultaneously offer rapid response times and the durability necessary to withstand the extreme conditions. Traditional methods, such as thermocouples and resistance temperature detectors, lack the requisite speed and durability for effective implementation in pulsed power systems or in scenarios characterized by rapid thermal fluctuations [8]. Consequently, the non-contact nature of optical thermometry approaches, like pyrometry and phosphor-based thermometry, could potentially offer the durability required for HEDP experiments. However, these approaches also face significant limitations. Pyrometry, for instance, is hampered by inadequate speed, low signal-to-noise ratios, and interference from plasma emissions [9]. Moreover, phosphor-based thermometry, despite offering a faster response, fails to accurately track temperature changes at gigahertz (GHz) rates. This limitation is largely due to the extended lifetimes of most phosphors and the issues arising from the deposition process, where the resultant film thickness (~ 4 μm) exacerbates thermal lag, further impeding the ability to capture rapid temperature dynamics effectively [10,11].

UP-SHOT bridges the existing gap in achieving rapid and precise temperature measurements under extreme conditions. This method capitalizes on the excitation ZnO thin films, deposited via atomic layer deposition (ALD), with ultrafast (fs) UV laser pulses. This technique's effectiveness is derived from utilizing the resulting photoluminescence (PL) of the free excitons in ZnO films to determine the temperature of the underlying sample or substrate. ZnO is an ideal material for UP-SHOT due to its wide bandgap, high melting point, short exciton lifetime, and robustness against irradiation [12-14].

Traditionally, ZnO has been used in phosphor thermometry as tracer particles [15-18]. The thermographic visible defect luminescence properties can be promoted when doped with excess zinc or gallium [16,19]. Additionally, ZnO has been shown to exhibit thermographic properties when doped with rare earth metals such as erbium (Er) or europium (Eu) [20,21]. For our specific application, the defect luminescence lifetimes in ZnO are too long, and doping ZnO with Er or Eu does not attain the necessary temperature ranges. Therefore, our research shifts the focus towards harnessing the UV excitonic emission of ZnO, which has proven to be effective for thermographic applications [15]. In addition, ZnO's high exciton binding energy (60meV) ensures the stability of free exciton even at elevated temperatures [22,23]. Using the excitonic emission allows us to exploit the shorter lifetimes of excitons—tightly bound electron-hole pairs—enabling a swift response to temperature fluctuations. Moreover, employing ALD for the deposition of ZnO thin films leverages the method's capability to create high-quality, ultra-thin films [24]. This feature crucially reduces thermal lag, significantly improving our ability to measure surface temperatures swiftly and accurately.

Furthermore, the fundamental excitonic properties of ZnO have been the subject of extensive research from cryogenic temperature to room temperatures [12,13,25-27]. This includes films deposited via ALD [28,29]. However, investigations into the behavior of free excitons above room temperature are more limited [22,23,30,31]. To the best of our knowledge, this study is the first to use time-resolved photoluminescence (TRPL) measurements to study both the effects of annealing in ZnO thin films at room temperature and to assess thermographic sensitivity at elevated temperatures, reaching up to approximately 250°C. Our findings indicate that ZnO maintains a short exciton lifetime under elevated temperatures, a crucial characteristic for the effective implementation of UP-SHOT. Thus, our work not only underscores its value for applications in high-speed optical thermometry but also enriches understanding of the fundamental lifetime dynamics of ZnO free excitons at elevated temperatures, offering valuable insights into their thermal behavior and lifetime.

DETAILED DESCRIPTION OF RESEARCH AND DEVELOPMENT AND METHODOLOGY:

2.1 Preparation of ZnO thin films by Atomic Layer Deposition and analysis

To achieve the desired thermal response characteristics, ZnO films were deposited to a target thickness of 55 nm using Atomic Layer Deposition (ALD), optimizing for minimal thermal lag and efficient exciton generation. The ALD process was conducted in a Cambridge NanoTech Savannah S100 chamber, utilizing Diethylzinc (DEZ, Strem Chemicals) and deionized water (18.5 megohm) as co-reactants. The process was facilitated by UHP argon (Matheson) serving as both the carrier and purge gas. Silicon (Si) (100) coupons (University Wafer) were prepared as substrates, undergoing a 10-minute ultraviolet-ozone treatment to ensure the removal of surface hydrocarbons. The deposition was carried out at 70°C and 150 °C. The growth rate of ZnO increases with deposition temperature. Additionally, a change in crystal orientation occurs at ~80 °C, which accentuates this trend at that temperature [32].

After deposition thickness was measured by spectroscopic ellipsometry (Woollam RC2), and surface roughness was measured by atomic force microscopy (AFM). Three independent areas of the wafer were imaged and mean and RMS values of roughness could be inferred. Values reported in the Results and Discussion are the average of the RMS and mean roughness values from the three images. Lastly, the crystallinity of the thin films produced was evaluated using x-ray diffraction (XRD) (Rigaku SmartLab II instrument). A Cu Kα source was used and operated at 44kV and 44mA. For XRD, the sample was aligned using a direct beam half cut sequence (z- and omega axes) and the diffractograms were acquired using a theta/2*theta scan with a step of 0.01 degrees.

2.2 Preparation of ZnO thin films by Aerosol Deposition and analysis

Additionally, an impact consolidation process, Aerosol Deposition (AD), was explored to build nanocrystalline coatings from commercial powders. Both ZnO:Zn powder and gallium doped zinc oxide (ZnO:Ga) powder were obtained from Phosphor Technology Ltd. The powders were characterized using XRD and Scanning Electron Microscopy. A memo outlining the preparation of the powder, the spray parameters, and the resulting coatings is included in Appendix A.

2.3 Annealing process

Post-deposition, the ZnO films underwent annealing to enhance UV emission characteristics and eliminate measurement hysteresis. The process involved an initial high-temperature step in ambient air to 500°C, 600°C, 700°C, 800°C, 900°C, and 1000°C; this produced thermal ramp rates of 95°C/min, 115°C/min, 135°C/min, 155°C/min, 175°C/min, and 195°C/min, respectively. A one hour anneal was performed, starting after the sample reached equilibrium with the oven. This process was selected because it aligns with the literature as being optimal for enhancing ZnO crystallinity without causing adverse phase or interfacial reactions [33,34]. A subsequent annealing step gradually increased the temperature to approximately 275°C for a duration of approximately 3 hours immediately before TRPL measurements. This second annealing process aimed at stabilizing the material states.

2.4 TRPL experimental setup

TRPL measurements were performed at the Center for Integrated Nanotechnologies (CINT). Figure 1 depicts the experimental setup, which consisted of a Coherent Chameleon 80 MHz Ti:Sapphire laser, generating 150 fs pulses at a central wavelength of 710 nm. These pulses were then frequency-doubled to 355 nm and directed perpendicularly onto the substrate surface at an incident power of 4.1mW, as measured by a Thorlabs power meter. Emissions were then detected by a Hamamatsu streak camera after going through a 375 nm longpass filter (Edmund Optics, #34-303), which was employed to eliminate extraneous laser light. Sample heating was achieved using a 24W ceramic heater (Thorlabs), insulated with Duraboard to minimize thermal losses. Temperature control and monitoring were facilitated by a Keithley 2400 power source, and a thermocouple embedded in the Duraboard, respectively.

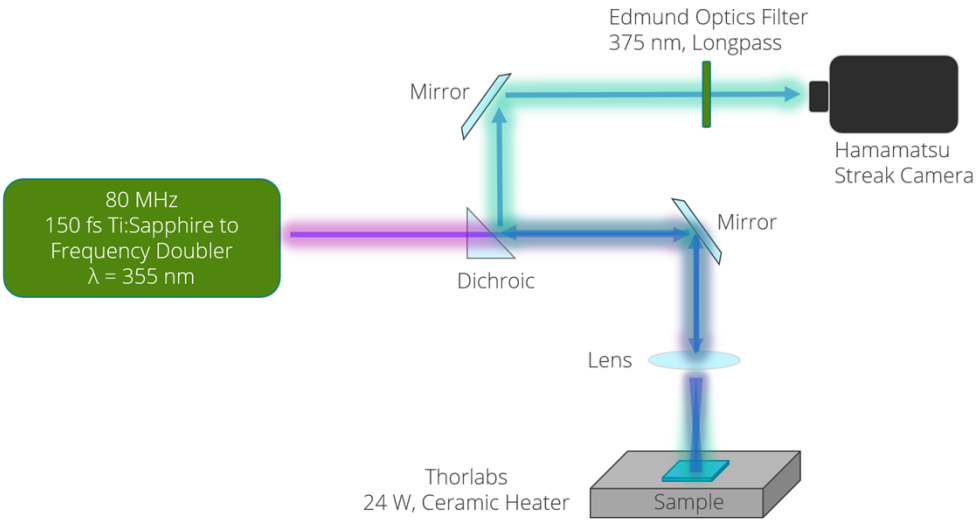

Figure 1. Schematic of the experimental setup for TRPL measurements.

2.5 TRPL data acquisition and analysis

Spectral intensity, peak shift, and emission lifetime were quantified through a streak camera with a gain setting of 10 and an integration time of 25s. Measurements commenced at room temperature and were incrementally increased in steps of approximately 30°C. Following temperature stabilization at each step, data were recorded up to a maximum of approximately 275°C.

Data were processed by two general methods: 1) *Integrated*- time or spectral integration was applied to the TRPL data to generate a single PL spectrum or luminescence trace, respectively; or 2) *Resolved*- each time-step or spectral bin within the TRPL data was processed independently.

Spectral peak locations and emission lifetime could be inferred using either method and are both used for traditional phosphor thermometry [35]. In the *Resolved* methodology, the mean peak wavelength and standard deviation were weighted by signal-to-noise (SNR_i) to correctly propagate uncertainty through the rise and decay of the exciton emission.

$$SNR_i = \frac{\mu_i}{\sigma_i} \quad \text{Eqn. 1}$$

Where the peak intensity, μ_i, is divided by the standard deviation of the noise, σ_i, at a given time step, i. For this work, the noise was taken from all data collected between 200 – 300nm, where no signal from either the excitation source or the exciton emission is expected.

The weighted mean peak wavelength, $\overline{\lambda}_{peak}$, is then calculated by weighting the peak wavelength, $\lambda_{peak,i}$, by the SNR_i at every time step:

$$\bar{\lambda}_{peak} = \frac{\sum_{i=1}^{N} SNR_i \lambda_{peak,i}}{\sum_{i=1}^{N} SNR_i} \quad \text{Eqn. 2}$$

Similarly, the weighted standard deviation,

$$\sigma_{SNR} = \sqrt{\frac{\sum_{i=1}^{N} SNR_i (\lambda_{peak,i} - \bar{\lambda}_{peak})^2}{\sum_{i=1}^{N} SNR_i}} \quad \text{Eqn. 3}$$

To infer the characteristic exciton lifetime, mean characteristic lifetime was inferred for each wavelength between 364 – 410 nm, and weighted via the inverse of the variance, assuming the standard deviation of the characteristic lifetime is estimated using the confidence intervals from the fitting routine. This wavelength range ensured that the photoluminescence trace of the spectral peak would be considered across all tested temperatures. An exponential fit, commonly applied for examining exciton dynamics in ZnO, was employed [38][39].

$$I(t) = A_1 e^{-\frac{t}{\tau}} \quad \text{Eqn. 4}$$

Where $I(t)$ is the intensity at time, t, A_1 is the amplitude, and τ is the characteristic lifetime of the emission decay. This model facilitated the extraction of decay constants at each temperature increment, which were then plotted against temperature to elucidate temperature-dependent exciton dynamics.

2.6 Static photoluminescence experimental setup

Measuring annealing effects on defect and exciton luminescence required static photoluminescence data. At room temperature, the Hamamatsu streak camera was run in 'static' mode to temporally integrate. This captured the short excitonic emission and the long-lived defect luminescence, which has a characteristic lifetime of ~1 µs [19]. A 375 nm longpass filter (Edmund Optics, #34-303), was employed to eliminate extraneous laser light.

RESULTS AND DISCUSSION:

3.1 As-deposited ZnO thin film characterization

The ALD process at 150°C growth temperature yielded ZnO thin films with a uniform thickness of 54.06 ± 1.75 nm, as confirmed by spectroscopic ellipsometry. A native SiO_2 layer of 1.7 nm was assumed for each sample that separates the Si wafer from the ZnO coating. For ultrafast thermometry, thermal lag within the coating must be considered, to ensure no erroneous biasing

of the measurement. The anticipated time for heat conduction propagation is taken by first considering the thermal diffusivity:

$$\alpha = \frac{k}{\rho c_p}, \quad \text{Eqn. 5}$$

For ZnO, the thermal conductivity, $k =$ 60 W/m·K, the density, ρ = 5600 kg/m³, and the specific heat, c_p= 490 J/kg·K. This results in a thermal diffusivity of $\alpha_{ZnO} \approx 2.18 \times 10^{-5} m^2/s$.

For SiO_2, the thermal conductivity, $k =$ 1.4 W/m·K, the density, ρ = 2200 kg/m³, and the specific heat, c_p= 703 J/kg·K. This results in a thermal diffusivity of $\alpha_{SiO} \approx 9.03 \times 10^{-7} m^2/s$.

The characteristic time for 1D heat conduction through a coating is estimated by:

$$t \approx \frac{L^2}{\alpha} \quad \text{Eqn. 6}$$

For ZnO, $t_{ZnO} \approx 1.34 \times 10^{-10} s$, where L = 54.06 $\times 10^{-9}$m; for SiO_2, $t_{SiO2} \approx 3.2 \times 10^{-12} s$, where L = 1.7 $\times 10^{-9}$m. The total mean characteristic time is $t \approx$ 137 picoseconds. The uncertainty introduced by variation in the ALD coating is accounted for considering the function, $t = f(L)$.

$$\Delta t \approx \left|\frac{\partial t}{\partial L}\right| \Delta L \quad \text{Eqn. 7}$$

$$\frac{\partial t}{\partial L} = \frac{\partial}{\partial L}\left(\frac{L^2}{\alpha}\right) = \frac{2L}{\alpha} \quad \text{Eqn. 8}$$

$$\Delta t \approx \left(\frac{2L}{\alpha}\right) \Delta L \approx 8.68 \times 10^{-12} s \quad \text{Eqn. 9}$$

Therefore, the characteristic time for heat conduction through the ALD ZnO coating is $(1.37 \pm 0.87) \times 10^{-10}$ s or 137 $\pm$ 87 picoseconds. An as-deposited coating of ZnO onto Si wafers will thermally respond to a linear thermal ramp of 19.5°C/nanosecond, with a thermal lag of 2.7°C within the 137 picosecond response time.

The average mean surface roughness of this as-deposited ZnO sample was R_{avg}= 0.76 nm, with a root mean square roughness of R_{RMS}= 0.85 nm; this indicates the initial coupons are relatively smooth, with minimal topological variation.

3.2 Treated ZnO thin film characterization

Different post-deposition annealing temperatures were investigated from 500 – 1000°C. The sample was introduced to heated ambient air and held for one hour. Photoluminescence spectra were taken after a post-anneal cool down back to 25°C.

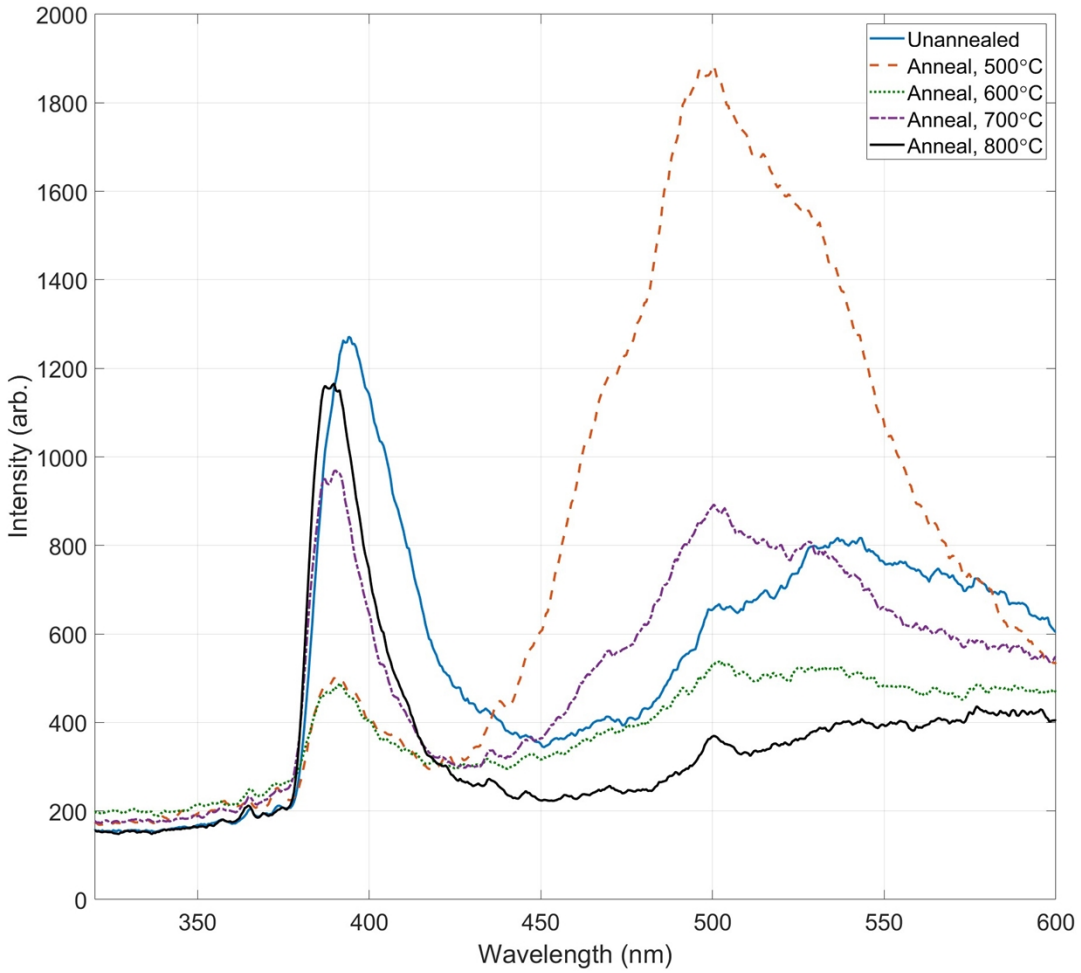

Figure 2: Comparison of the photoluminescence from ALD ZnO deposited onto silicon wafers at a growth temperature of 70°C annealed in air for one hour at different temperatures to the unannealed, as-deposited samples. Spectra were taken with 355 nm excitation light over 25s integration time.

This static PL data elucidates the improvements of annealing the ZnO on Si wafers. The unannealed sample produced both exciton emission (~370 nm) and defect luminescence (420 – 600 nm). Annealing at 500°C greatly enhanced the defect luminescence, indicating the formation

of additional defects within the lattice. Ambient air was chosen over an inert environment to try and provide oxygen to the ZnO coating and limit the formation of oxygen vacancies and interstitial zinc. At 600°C both excitonic emission and defect luminescence were suppressed before both began to recover after annealing at 700°C. A post-deposition annealing at 800°C significantly enhanced the crystallinity of the ZnO films as confirmed by room temperature PL and XRD measurements. The excitonic peak blue shifted; note that the longpass filter didn't influence the peak, there is an effect on the spectral lineshape. The XRD is shown in Figure 3.

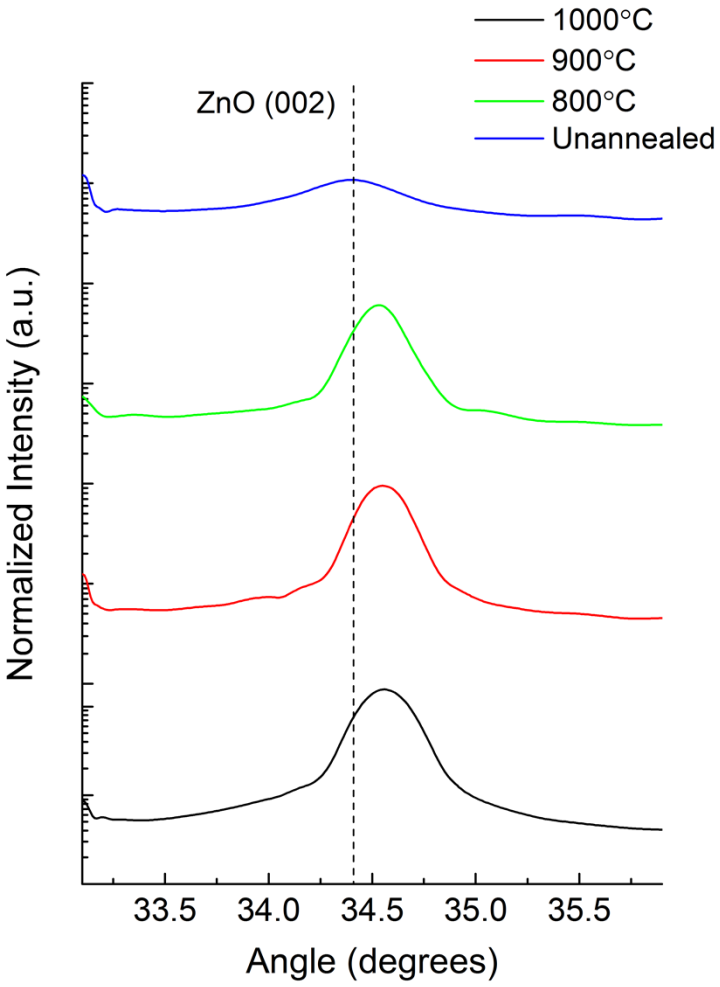

Figure 3: XRD of the (002) ZnO peak. With increased annealing temperature, the peak narrows and intensifies, indicating improved crystallinity.

Between the unannealed and the 800°C sample, there are two notable effects: 1) the full width half maximum (FWHM) of the peak narrows and 2) the peak shifts to higher angles. This indicates improved crystallinity and a shift towards a smaller lattice parameter, respectively.

An 800°C anneal of ALD ZnO grown at 150°C produced similar behavior. A subsequent annealing step at 275°C immediately before TRPL measurements further stabilized the material states, preparing the films for high-temperature TRPL analysis, which was shown by very little change in PL wavelength and integrated before and after temperature testing.

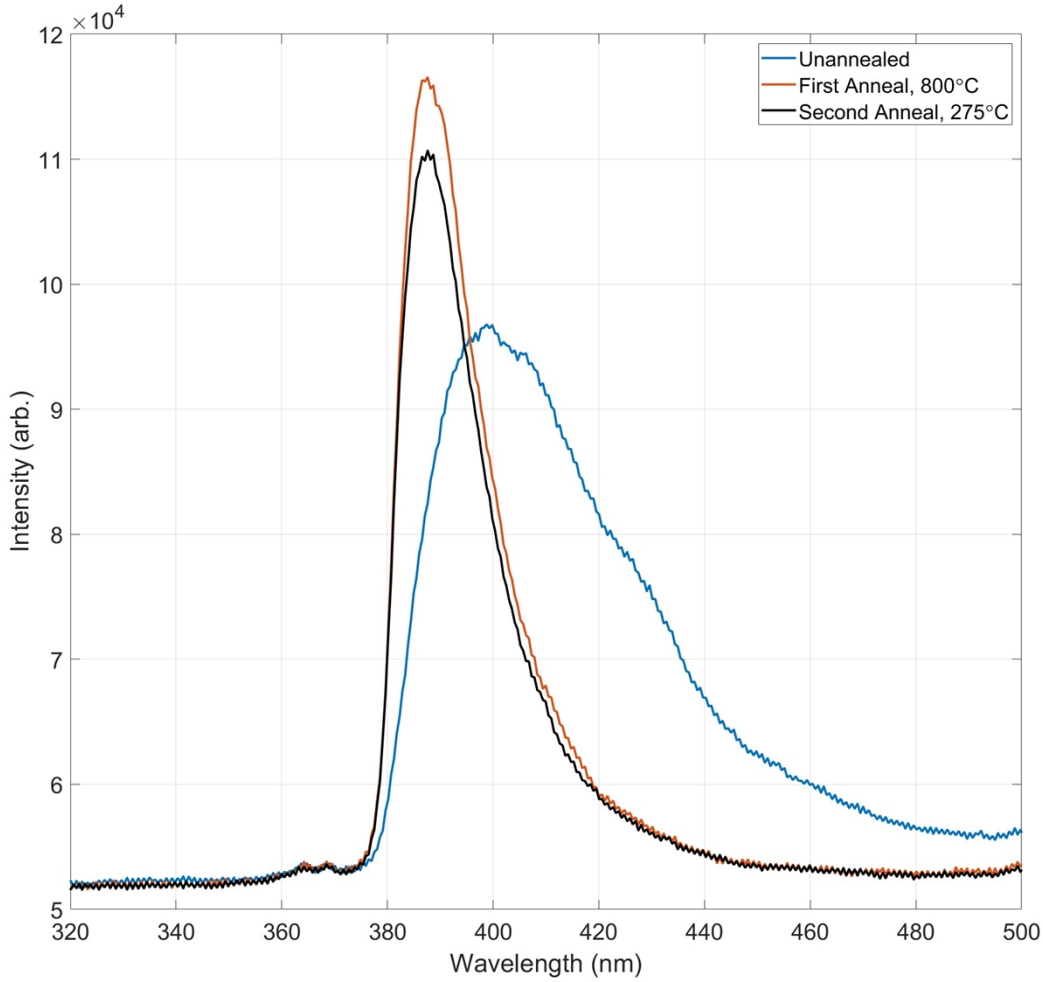

Figure 4: Photoluminescence spectra with excitation wavelength (355 nm), of ALD deposited ZnO on silicon wafers at 150°C growth temperature in the as-deposited (blue), annealed (black), and double-annealed (orange) treatments.

Annealing also changed both the coating thickness and roughness, as measured by spectral ellipsometry and AFM. Table 1 provides a comparison between the as-deposited and annealed values for ZnO samples grown at 70°C, and the thermal lag expected from each sample.

Table 1: Comparison of coating properties of ALD ZnO deposited on Si wafers at 70°C, after different annealing treatments

Sample Anneal	Mean Roughness (nm)	RMS Roughness (nm)	Average Thickness (nm)	STD Thickness (nm)	Thermal Lag (°C)
As-deposited	1.3	1.8	53.1	2.3	2.5
500°C	5.3	8.4	56.4	0.5	2.8
600°C	2.5	3.2	54.9	0.5	2.7
700°C	2.9	4.1	58.5	0.2	3.1
800°C	2.8	3.7	59.1	0.03	3.1
900°C	3.2	4.1	75.2	0.1	5.1
1000°C	13.8	17.2	91.0	0.3	7.4

A significant increase in thickness and roughness were measured at annealing temperatures of 900°C and 1000°C. This corresponded with a significant increase in luminescence. At this time, it has not been established if this increase is due to improved quantum efficiency or additional luminescing material. We hypothesize that defected Zn_2SiO_4 was formed at the interface between the native SiO_2 layer and the ZnO coating. Oxygen from the ZnO lattice can migrate, producing oxygen vacancy defects. Since these samples were annealed in ambient air, gaseous oxygen may be present to fill those vacancies. XRD established silicate formation at 1000°C, as shown in Figure 5.

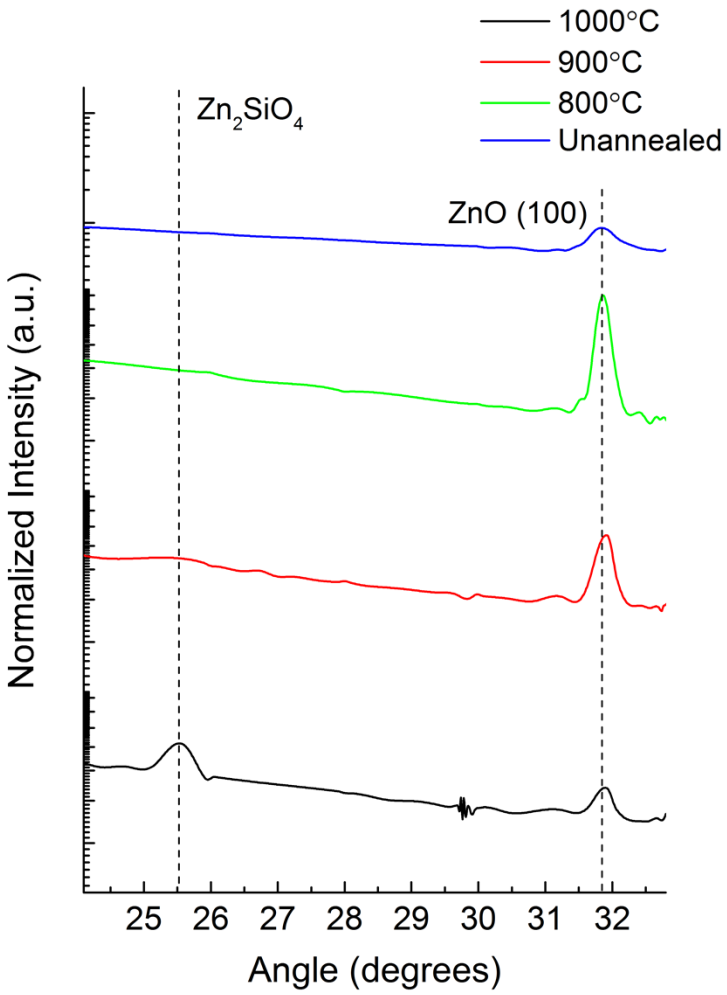

Figure 5: XRD of the ZnO (100) peak and Zn_2SiO_4 for the unannealed and high annealing temperatures.

Interestingly, the ZnO(100) peak intensity increases at 800°C and then decreases from there to 1000°C. There are no significant shifts in the peak angle. However, a new zinc silicate peak is clearly visible at the highest annealing temperature. Further study of the interface between ZnO and Si is required, including a measurement of quantum efficiency.

4.1 TRPL results

The TRPL setup, utilizing a tunable 80 MHz Ti:Sapphire laser with pulses frequency-doubled to 355 nm, facilitated precise temperature measurements on the ZnO films. Temperature increments of approximately 30°C were applied, starting from room temperature and progressing to a maximum of 275°C. The spectral intensity, shift, and emission lifetime data were meticulously

recorded at each temperature step. Figure 6 compares the spectra integrated over the full emission lifetime.

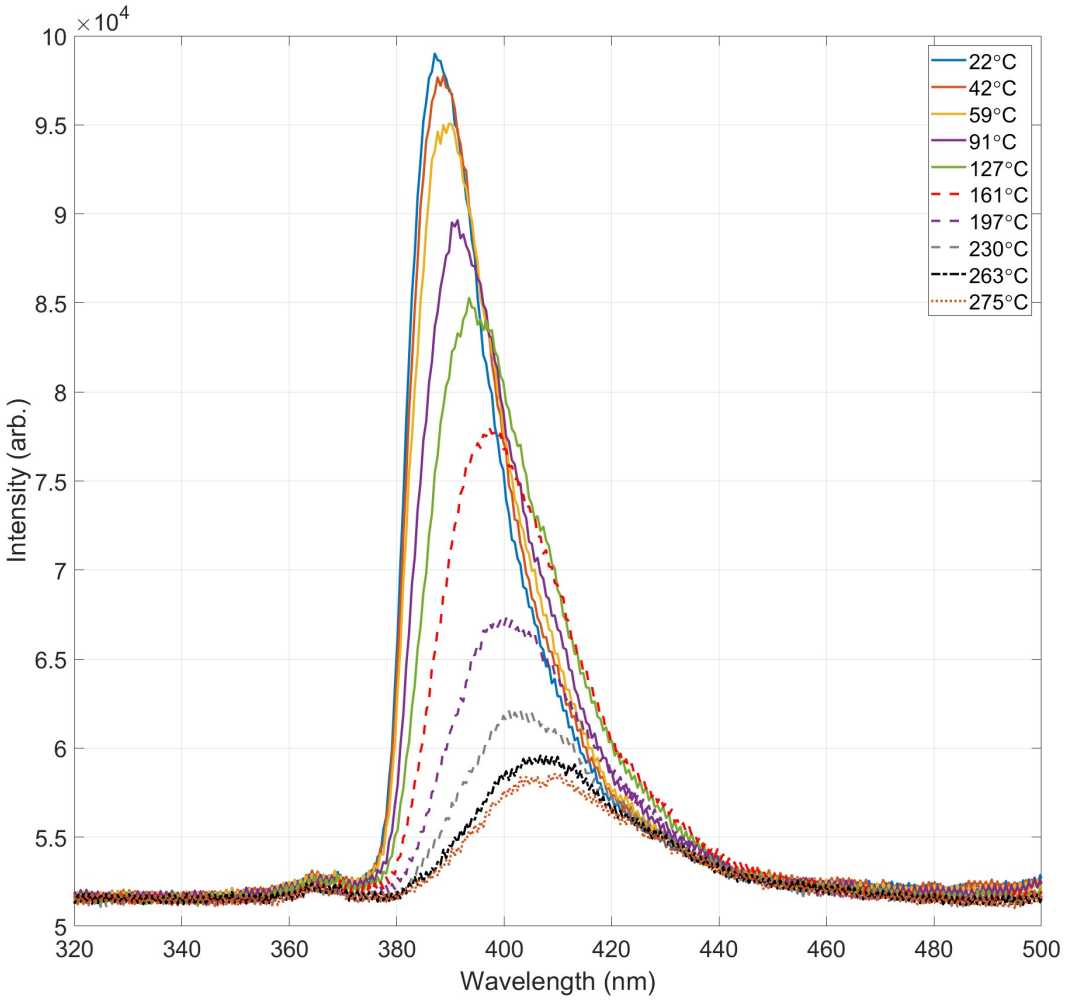

Figure 6: Spectral data integrated across all time steps from a TRPL trace of 150°C ZnO grown on Si wafers and annealed at 800°C held at different prescribed temperatures.

Notably, the excitonic intensity and spectral peak location change. This is further explored in Figure 7. The peak wavelength exhibited a consistent shift with temperature, indicating a direct correlation between the photoluminescence properties of ZnO and the substrate temperature. This is consistent with previous work [14].

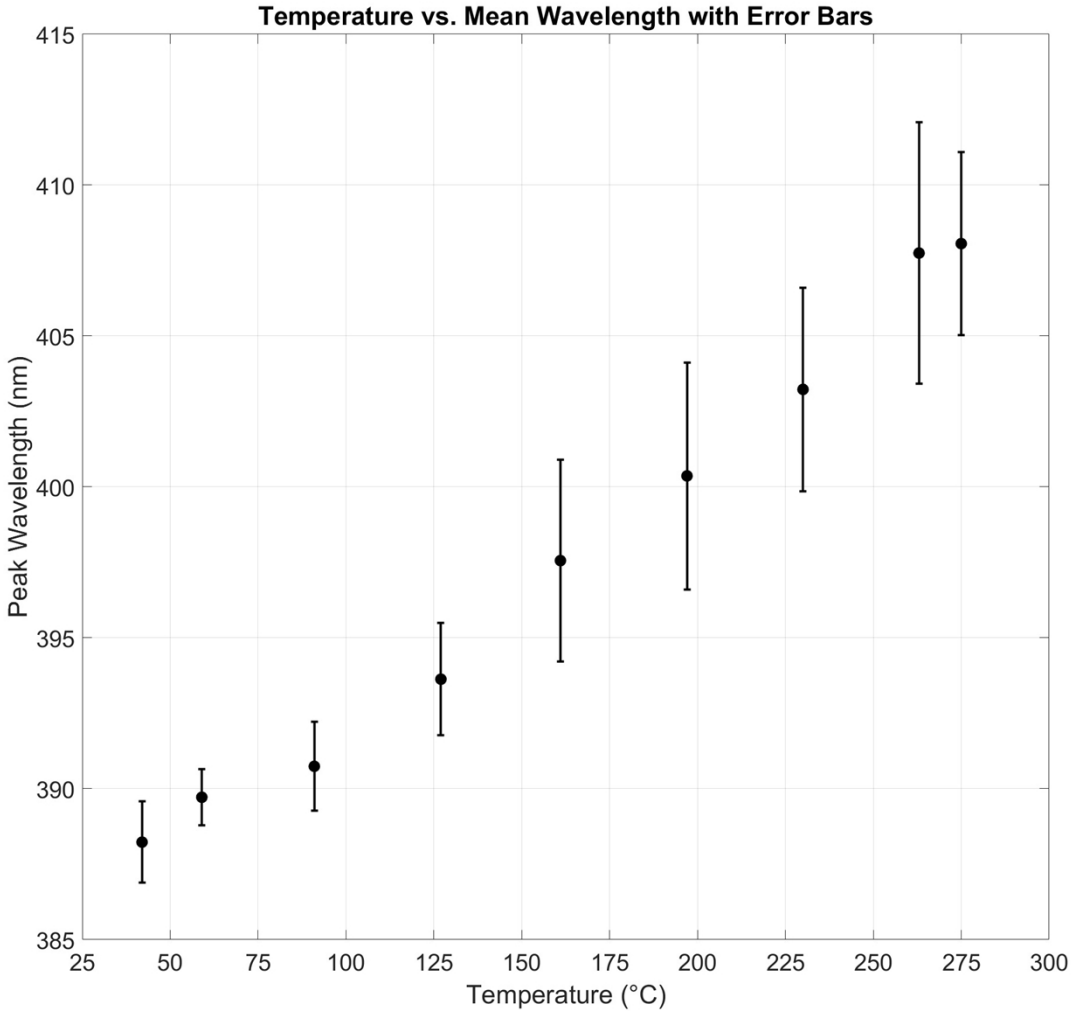

Figure 7: The mean spectral peak of ZnO exciton emission from 150°C ZnO grown on Si wafers annealed at 800°C held at different prescribed temperatures.

A linear regression fit of the data in Figure 7 estimates the thermographic sensitivity of peak wavelength to temperature to be 0.084±0.003 nm/°C, which is in good agreement with the sensitivity estimated from prior work ≈ 0.10 nm/°C [14]. The linear regression was weighted by the variance of each data point.

The excitonic lifetime was inferred across the participating free-excitonic wavelengths. The wavelength binning was every 0.513 nm.

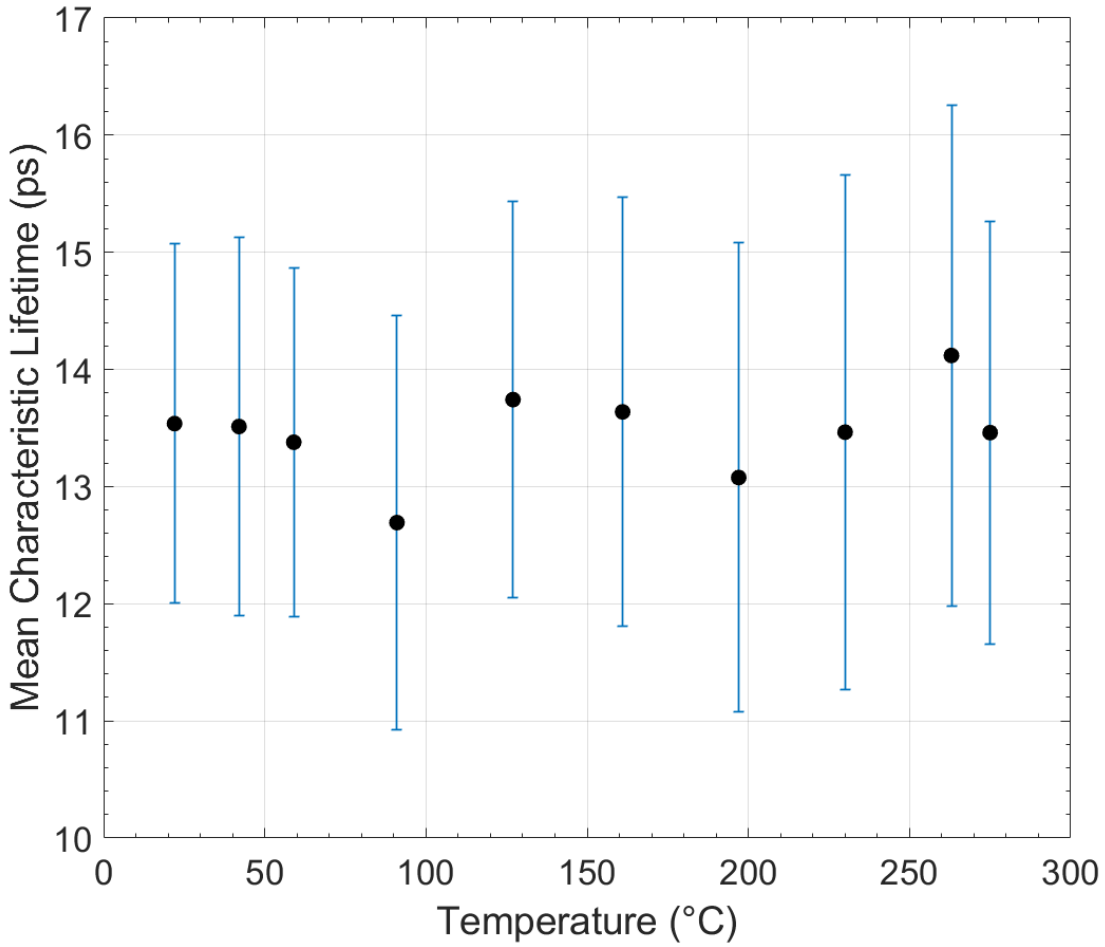

Figure 8: Lifetimes inferred from the time-resolved luminescence at the spectral peak for each temperature. A bi-exponential fit was used to collect both the band-edge and free excitonic emission.

The characteristic excitonic lifetime is always less than 17 ps and is not thermographic at these temperatures. These analyses are crucial for the effectiveness of UP-SHOT, as it ensures rapid and accurate temperature measurements without significant delay.

ANTICIPATED OUTCOMES AND IMPACTS:

4.1 Next Steps

UP-SHOT successfully developed a new ultra-fast thermometry capability, with an eye towards capturing the physics of power deposition on HEDP experiments. This exploratory project has been further funded for FY25 and FY26 to continue development.

Next steps include in-situ calibration on the benchtop to exercise UP-SHOT at different heating rates. Laser heating of an insulated sampled will be targeted to vary pulse duration and therefore prove out UP-SHOT at MHz-GHz data acquisition rates.

Optical design to match the facility constraints has been completed. Next steps include building an excitation system to split a single beam into up to four individual pulses and delay them by nanoseconds to capture GHz phenomena. When designing the beam line, we must consider the laser fluence on the specimen, to maximize signal-to-noise without additional heating, the time of the pulses, data processing of GHz signals, and accurate temperature inference.

The temperature sensitivity of UP-SHOT was initially quantified considering the spectral peak shift to be $\approx$ 0.084 nm/°C. An improved figure of merit will be considered to account for signal-to-noise from the specimen, and the convolution of systematic resolving power. There are two paths forward to implementing UP-SHOT: time-resolved and time-integrated thermometry. Time resolved thermometry, is similar to the TRPL reported. The spectral peak of the exciton would be monitored throughout each measurement. This requires streak visible spectroscopy (SVS). SVS is beneficial to monitor stray light interference and record data throughout an entire heating event. However, time-resolved thermometry produces lower signal-to-noise. Time-integrated thermometry would acquire all photons within a specific bandpass over measurement time. This inherently increases the signal-to-noise but can limit that thermographic sensitivity and dynamic range. Both options will be considered and compared.

Finally, this work established the temperature dependence of the ZnO coatings. However, within HEDP experiments, there are coupled effects between the temperature, electric, and magnetic fields. Follow-on funding will explore the spectral effects of electric fields on ZnO.

4.2 Anticipated Publications

FY24 work has yielded two journal manuscript drafts. One manuscript will describe the UP-SHOT diagnostic and the deposition and characterization of ultra-thin ZnO coatings. The second manuscript will document the high temperature annealing of ZnO on Si that resulted in interesting interface dynamics.

4.3 Conference Presentation

UP-SHOT was shared with the diagnostics community during the Laser Applications to Chemical, Security, and Environmental Analysis (LACSEA), a co-located conference within the Optical Congress hosted by OPTICA. Caroline Winters presented a conference presentation, served as a Program Chair for LACSEA, and will continue to serve as a General Chair.

Noelle Collins presented UP-SHOT as a poster for the 2024 Center for Integrated Nanotechnologies Annual Meeting. Noelle is a current graduate student at the University of New Mexico. This work supports her PhD thesis.

4.4 New R&D and IP Development:
This project has produced two Technical Advances: *Ultrafast Phosphor Surface Heating Optical Thermometry (UP-SHOT)* and *Method for Enhancing Photoluminescence in ZnO Thin Films via Interface Engineering.*

4.5 Impact and path forward for NNSA and DOE
UP-SHOT is a transformational project. This minimally invasive diagnostic discovers if phosphor thermometry captures GHz phenomena, opening the door for advanced surface thermometry in Z and future efforts to extend phosphor functionality towards extreme electro-magnetic environments. This LDRD designed a diagnostic to capture surface heating related to thermal desorption and melting behaviors common to HEDP experiments to inform the physical understanding of plasma initiation, energy loss mechanisms, and material thermal response.

New, temporally resolved and minimally intrusive thermometry capabilities that can survive extreme electrical, thermal, and mechanical environments will increase agility in design for NGPP. The accuracy and initial sensitivity of the diagnostic has been inferred, and will be demonstrated during dynamic, high-energy deposition heating of materials. We offer quantitative measurements useful for boundary and interface conditions with minimal interference from the testing environment to improve confidence in model validation.

Even if full implementation is not possible, the benchtop work on material science for UP-SHOT is directly transformational towards the applicability of wide-bandgap semiconductor materials in extreme environments.

This project is beneficial to advancing the Laboratories Strategic Priorities: (1) Fulfilling Commitments to our customers by discovering a new diagnostic capability for current and next-generation pulsed-power facilities; (2) Engineering, Science and Technology in developing a cutting edge thermometry diagnostic to serve mission goals; and (3) Unleashing the Power of Sandia by providing quantitative boundary condition measurements of hardware in a new way, promoting faster design cycles and improved confidence in modeling and validation.

CONCLUSION:

UP-SHOT is a synergistic coupling of advanced manufacturing, material physics, and optical engineering. For ALD ZnO deposited on Si wafers, a post-deposition anneal produced improved crystallinity and excitonic signal, optimized at 800°C in ambient air. Annealing up to 800°C did evolve the coating properties, increasing the thickness by 6 nm; it is inferred this will result in a thermal lag of 3.2°Cover the thermal response time. Previous work noted ZnO:Zn powder produced a thermographic spectral peak sensitivity $\approx$ 0.10 nm/K [14], which is in good agreement with UP-SHOT's measured spectral peak sensitivity $\approx$ 0.084 nm/K.

Above 800°C, annealing ZnO on Si begins to produce defected Zn_2SiO_4, at the interface between the native SiO_2 layer and the ALD ZnO. This was confirmed via XRD. The resulting process increased both the coupon thickness and the luminescence signal.

The results of this project validate the UP-SHOT technique as a significant advancement in the field of optical thermometry. By leveraging the unique properties of ZnO thin films, UP-SHOT paves the way toward nanosecond precision in elevated temperature measurements. Furthermore, we demonstrate for the first time at the best of our knowledge, TRPL of ZnO thin films at elevated temperatures, which confirmed that exciton lifetimes remain short, and therefore useful for high-speed thermometry at these temperatures. This breakthrough opens new avenues for research and applications in high-speed, high-temperature environments, establishing UP-SHOT as a significant development in temperature measurement technology.

ACKNOWLEDGEMENTS:

The authors would like to acknowledge the contributions from Professor Daniel Feezell of the University of New Mexico and Drs. Prashant Padmanabhan and Igal Brener from the Center for Integrated Nanotechnologies during this project. Additionally, the authors acknowledge Dr. Charles Rose as a lead in the conception of UP-SHOT.

REFERENCES:

[1] Bennett, N., Welch, D. R., Jennings, C. A., Yu, E., Hess, M. H., Hutsel, B. T., ... & Cuneo, M. E. (2019). Current transport and loss mechanisms in the Z accelerator. Physical Review Accelerators and Beams, 22(12), 120401.

[2] Laity, G. R., Robinson, A. C., Cuneo, M. E., Alam, M. K., Beckwith, K. R., Bennett, N. L., ... & Smith, T. J. (2021). Towards Predictive Plasma Science and Engineering through Revolutionary Multi-Scale Algorithms and Models (No. SAND2021-0718). Sandia National Lab.(SNL-NM), Albuquerque, NM (United States); Sandia National Laboratories, SNL California.

[3] Fangohr, H., Chernyshenko, D. S., Franchin, M., Fischbacher, T., & Meier, G. (2011). Joule heating in nanowires. Physical Review B, 84(5), 054437.

[4] Oreshkin, V. I., Chaikovsky, S. A., Labetskaya, N. A., Datsko, I. M., Rybka, D. V., Ratakhin, N. A., & Khishchenko, K. V. (2015, November). Nonlinear diffusion waves in high magnetic fields. In Journal of Physics: Conference Series (Vol. 653, No. 1, p. 012143). IOP Publishing.

[5] Matzen, M. Keith, et al. "Pulsed-power-driven high energy density physics and inertial confinement fusion research." Physics of Plasmas 12.5 (2005).

[6] Sinars, D. B., et al. "Review of pulsed power-driven high energy density physics research on Z at Sandia." Physics of Plasmas 27.7 (2020).

[7] Savage, M. E., et al. "An overview of pulse compression and power flow in the upgraded Z pulsed power driver." 2007 16th ieee international pulsed power conference. Vol. 2. IEEE, 2008.

[8] Dinh, Toan, et al. "Thermoresistive effect for advanced thermal sensors: Fundamentals, design considerations, and applications." Journal of Microelectromechanical Systems 26.5 (2017): 966-986.

[9] Kostkowski, Henry J., and Richard Dean Lee. Theory and methods of optical pyrometry. No. 41. US Department of Commerce, National Bureau of Standards, 1962.

[10] Fuhrmann, N., et al. "High-speed phosphor thermometry." Review of Scientific Instruments 82.10 (2011).

[11] Brübach, Jan, et al. "On surface temperature measurements with thermographic phosphors: a review." Progress in Energy and Combustion Science 39.1 (2013): 37-60.

[12] Litton, Cole W., Donald C. Reynolds, and Thomas C. Collins. "Zinc oxide materials for electronic and optoelectronic device applications." (2011).

[13] Rasmidi, Rosfayanti, Mivolil Duinong, and Fuei Pien Chee. "Radiation damage effects on zinc oxide (ZnO) based semiconductor devices–a review." Radiation Physics and Chemistry 184 (2021): 109455.

[14] Janotti, Anderson, and Chris G. Van de Walle. "Fundamentals of zinc oxide as a semiconductor." Reports on progress in physics 72.12 (2009): 126501.

[15] Abram, C., Fond, B., & Beyrau, F. (2015). High-precision flow temperature imaging using ZnO thermographic phosphor tracer particles. Optics express, 23(15), 19453-19468.

[16] Kopf, A., Frattina, V., Bardi, M., Endres, T., Bruneaux, G., & Schulz, C. (2023). In-cylinder thermographic PIV combined with phosphor thermometry using ZnO: Zn. International Journal of Engine Research, 24(1), 113-131.

[17] Fan, L., Gao, Y., Hayakawa, A., & Hochgreb, S. (2017). Simultaneous, two-camera, 2D gas-phase temperature and velocity measurements by thermographic particle image velocimetry with ZnO tracers. Experiments in Fluids, 58, 1-12.

[18] Abram, C., Pougin, M., & Beyrau, F. (2016). Temperature field measurements in liquids using ZnO thermographic phosphor tracer particles. Experiments in Fluids, 57, 1-14.

[19] Särner, Gustaf, Mattias Richter, and Marcus Aldén. "Two-dimensional thermometry using temperature-induced line shifts of ZnO: Zn and ZnO: Ga fluorescence." Optics letters 33.12 (2008): 1327-1329.

[20] Jahanbazi, Forough, and Yuanbing Mao. "Recent advances on metal oxide-based luminescence thermometry." Journal of Materials Chemistry C 9.46 (2021): 16410-16439.

[21] Senapati, Subrata, and Karuna Kar Nanda. "Ultrahigh-sensitive optical temperature sensing based on quasi-thermalized green emissions from Er: ZnO." Physical Chemistry Chemical Physics 19.3 (2017): 2346-2352.

[22] Chen, Xiang-Bai, et al. "The properties of ZnO photoluminescence at and above room temperature." Journal of Applied Physics 102.11 (2007).

[23] Margueron, Samuel, and David R. Clarke. "The high temperature photoluminescence and optical absorption of undoped ZnO single crystals and thin films." Journal of Applied Physics 116.19 (2014).

[24] Tynell, Tommi, and Maarit Karppinen. "Atomic layer deposition of ZnO: a review." Semiconductor Science and Technology 29.4 (2014): 043001.

[25] Hopfield, J. J. "A theory of edge-emission phenomena in CdS, ZnS and ZnO." Journal of Physics and Chemistry of Solids 10.2-3 (1959): 110-119.

[26] Thomas, D. G. "The exciton spectrum of zinc oxide." Journal of Physics and Chemistry of Solids 15.1-2 (1960): 86-96.

[27] Wagner, M. R., et al. "Bound excitons in ZnO: Structural defect complexes versus shallow impurity centers." Physical Review B—Condensed Matter and Materials Physics 84.3 (2011): 035313.

[28] Beh, Holger, et al. "Photoluminescence dynamics and quantum yield of intrinsically conductive ZnO from atomic layer deposition." Journal of Luminescence 201 (2018): 85-89.

[29] Przeździecka, E., et al. "Photoluminescence, electrical and structural properties of ZnO films, grown by ALD at low temperature." Semiconductor Science and Technology 24.10 (2009): 105014.

[30] Rai, R. C. "Analysis of the Urbach tails in absorption spectra of undoped ZnO thin films." Journal of Applied Physics 113.15 (2013).

[31] Bagnall, D. M., et al. "High temperature excitonic stimulated emission from ZnO epitaxial layers." Applied Physics Letters 73.8 (1998): 1038-1040.

[32] Malm, J., Sahramo, E., Perälä, J., Sajavaara, T., & Karppinen, M. (2011). Low-temperature atomic layer deposition of ZnO thin films: Control of crystallinity and orientation. *Thin Solid Films*, *519*(16), 5319-5322.

[33] Xu, Xiaoliang, et al. "Annealing effect for surface morphology and luminescence of ZnO film on silicon." Chemical physics letters 364.1-2 (2002): 57-63.

[34] Zheng, Hua, et al. "Thickness-dependent optical constants and annealed phase transitions of ultrathin ZnO films." The Journal of Physical Chemistry C 120.39 (2016): 22532-22538.

[35] Fuhrmann, N., J. Brübach, and A. Dreizler. "Phosphor thermometry: A comparison of the luminescence lifetime and the intensity ratio approach." Proceedings of the Combustion Institute 34.2 (2013): 3611-3618.

[36] Wischmeier, L., et al. "Dynamics of surface-excitonic emission in ZnO nanowires." Physical Review B—Condensed Matter and Materials Physics 74.19 (2006): 195333.

[37] Van Dijken, Addy, et al. "The kinetics of the radiative and nonradiative processes in nanocrystalline ZnO particles upon photoexcitation." The Journal of Physical Chemistry B 104.8 (2000): 1715-1723.

APPENDIX A: AEROSOL DEPOSITION

This appendix summarizes the deposition of ZnO:Zn and ZnO:Ga using aerosol deposition for the *Ultrafast Surface Phosphor Thermometry for Pulsed-power and Hostile Environments* project. The goal was to produce samples for signal testing. The aerosol deposition work was performed at SNL/NM at the Thermal Spray Research Laboratory.

Substrates

The substrates for the ZnO:Zn runs were aluminum Almen strips purchased from Electronics inc. (grade AA 999202, 2024-T3 Al, 3 x 0.75 x 0.032 inches). The substrates for the ZnO:Ga runs were annealed stainless steel strips obtained from TBI (430 ANNLD SS, size 0.25, part C-3/443012-25, 0.75 x 0.5 inch). All of the substrates were cleaned with acetone, IPA, then distilled water.

Powders

The ZnO:Zn powder was obtained from Phosphor Technology Ltd. (product GK30/F-F1, 3.5-micron particle diameter, AQ40303491, lot 26200). X-ray diffraction (XRD) performed by Nichole Valdez confirmed the purity of the powder as single phase ZnO, as seen in Figure A1.

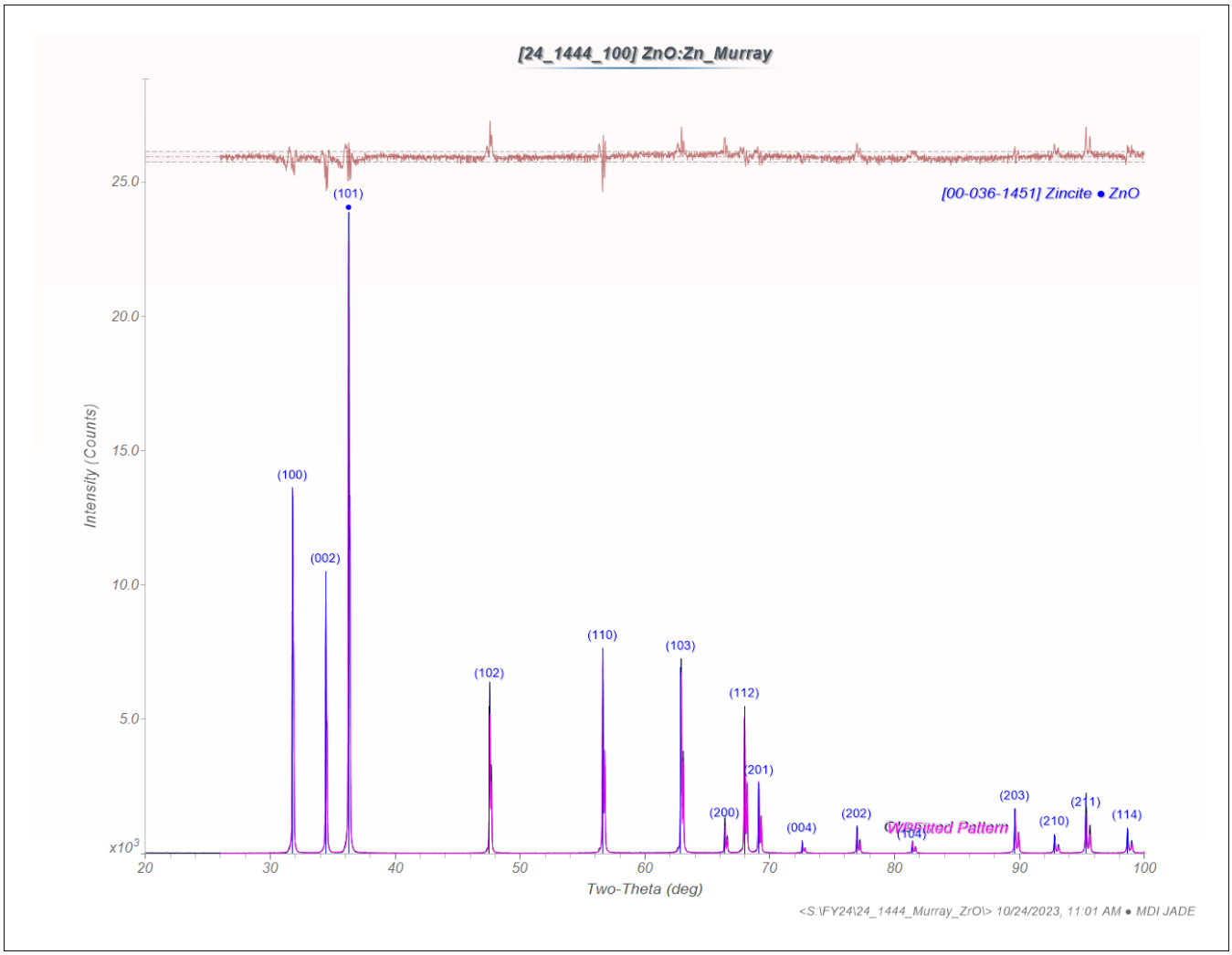

Figure A1: X-ray diffraction results for the ZnO:Zn as-received powder.

The ZnO:Ga powder was also obtained from Phosphor Technology Ltd. (product GK31/S-S1, 5-micron particle diameter, AQ40407697, lot 32166). XRD confirmed the purity of the ZnO:Ga, as seen in Figure A2. The powder is phase pure with a Zincite structure. The unit cell has expanded due to the doping.

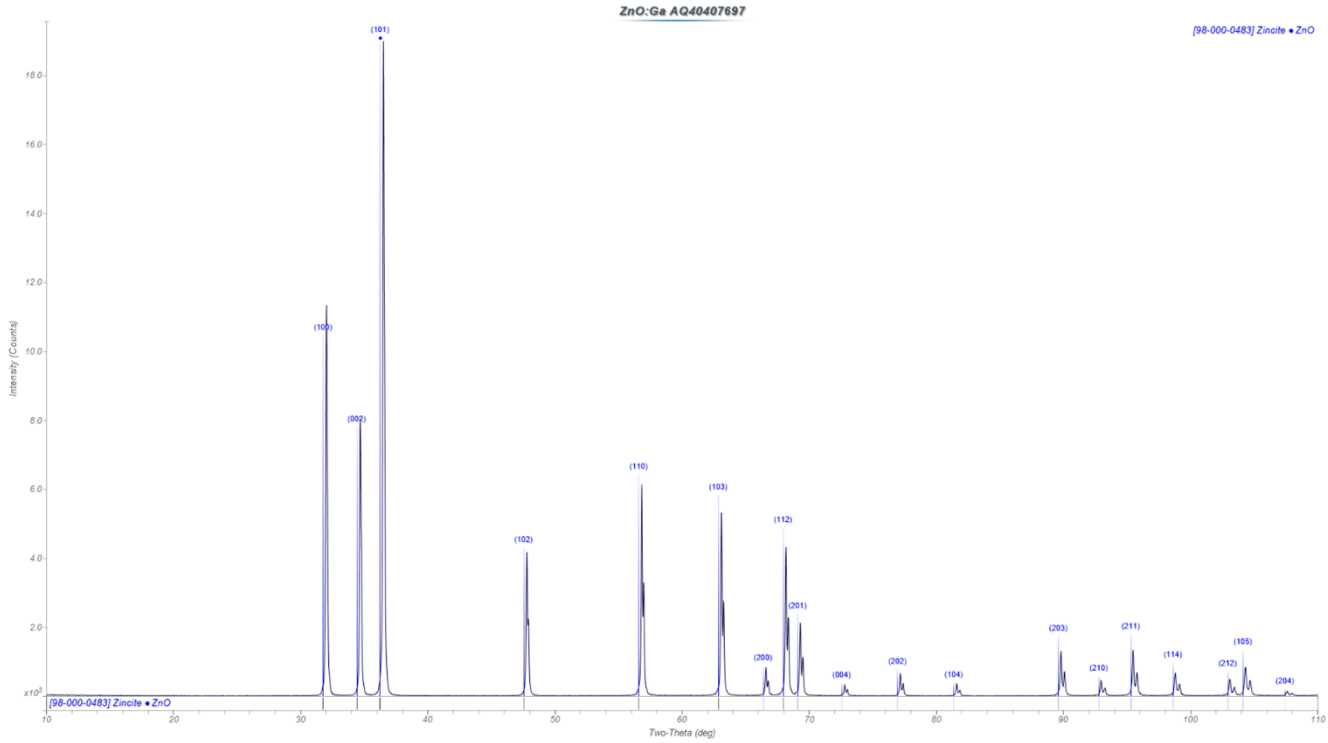

Figure A2: X-ray diffraction results for the ZnO:Ga as-received powder.

To prepare the powders for use with AD, the powders were ball milled using a Fritsch Pulverisette 7 high energy planetary mill. Each milling bowl was filled with 70 g of 1 mm diameter spherical, zirconia media and a slurry containing 20 g of powder mixed with 22 g of distilled water. The slurry was milled at 850 revolutions per minute for 5 minutes on, and 20 minutes off, with no reverse for 10 cycles. The milled slurry was rinsed into a container using distilled water and dried for 24 hours at 150°C. Both as-received powders are white. But after ball milling, both powders were a light-yellow color. A picture of the ZnO:Zn powder before and after ball milling is given in Figure A3.

Figure A3: Picture of the ZnO:Zn, as-received, in the bottle (right) and after ball milling (left). The ball milled powder was a light-yellow color while the as-received powder was white.

Scanning electron microscope (SEM) images of the as-received and ball milled ZnO:Ga are shown in Figure A4. Both powders have large agglomerates, but the ball milled powder has a smaller primary particle size. The process of ball milling the powder in water and drying it is known to produce soft agglomerates, which is why it is ground and sieved. But some agglomerates remain since a 180-micron sieve is used.

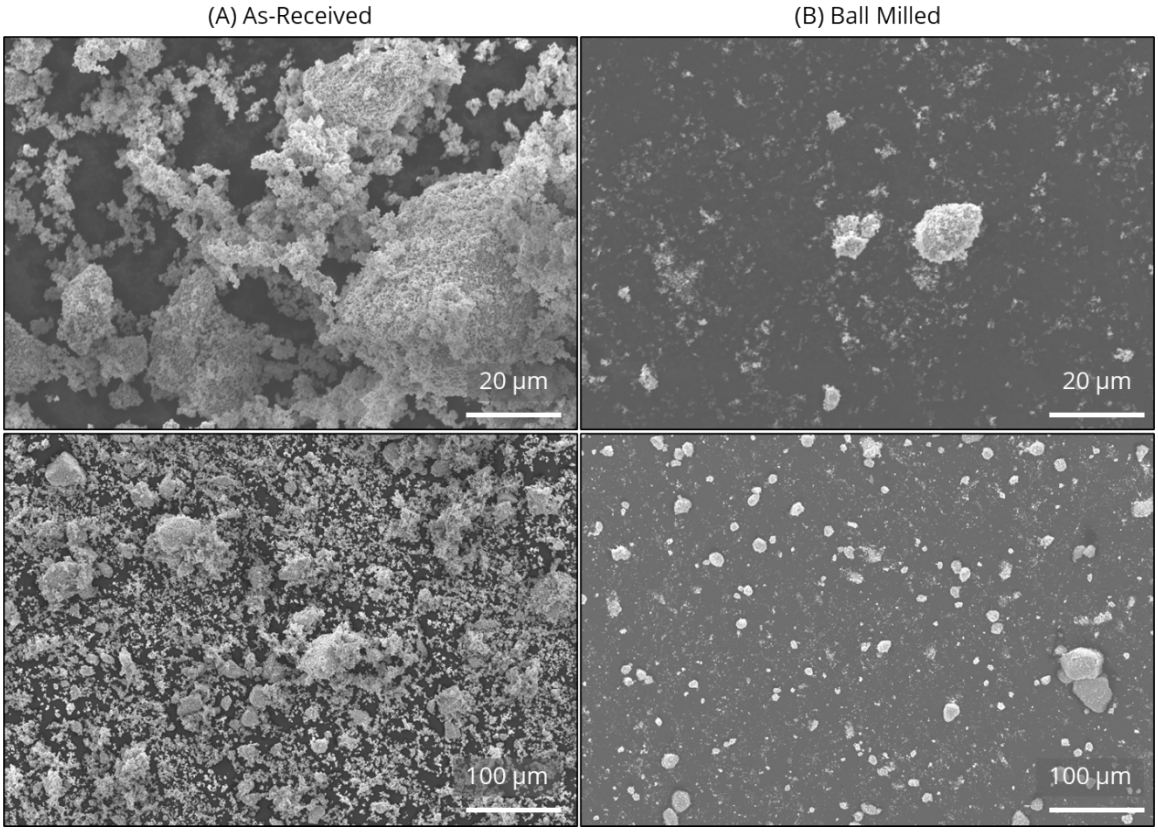

Figure A4: SEM images of the (A) as-received and (B) ball milled ZnO:Ga powder.

Characterization

The powder was imaged using a JEOL JCM-6000Plus Benchtop SEM. A Keyence VK-X150 Laser Profilometer was used to measure the thickness of the coatings. Powder X-ray diffraction data was collected on a Siemens D500 Kristalloflex system equipped with a sealed tube X-ray source (Cu Ka radiation), a diffracted-beam graphite monochromator, and a scintillation detector. Power settings for X-ray generation were 40 kV and 30 mA. The scan range was 10-100° 2q with a step size of 0.02° 2q and a dwell time of 10.0 seconds. XRD data was processed in JadePro version 8.7 (Materials Data, Inc.) with the PDF-4+ Database for phase ID. Whole pattern fitting was performed to estimate the doped unit cell lattice parameters of the ZnO:Ga

sample. For ZnO:Zn, whole pattern fitting was performed to estimate the lattice parameters of the ZnO phase, which were very close to the database pattern (PDF-# 04-003-2106).

Experimental Setup

The aerosol deposition (AD) system used at the Thermal Spray Research Laboratory (TSRL) is described in 0 and 0 but also summarized here. A Palas GmbH, RBG1000isd rotating brush generator (RBG) is used to aerosolize the powder. The feedstock powder is packed into the piston, which is fed at a constant rate into the rotating brush. Helium gas flows over the brush aerosolizing the powder. The aerosolized powder is then accelerated through a 3D printed Vero polymer converging-diverging nozzle into a vacuum chamber where the particles impact the substrate and build up the coating. A vacuum chamber is required to accelerate the He carrier gas through the nozzle and ensure the feedstock powder reaches the substrate at a sufficient velocity for deposition.

Spray Configuration

The runs were performed using the classic configuration for AD. The nozzle is fixed and pointing upwards while the x-y stage rasters the substrate over the nozzle. A labeled picture of the setup within the AD vacuum chamber is shown in Figure A5.

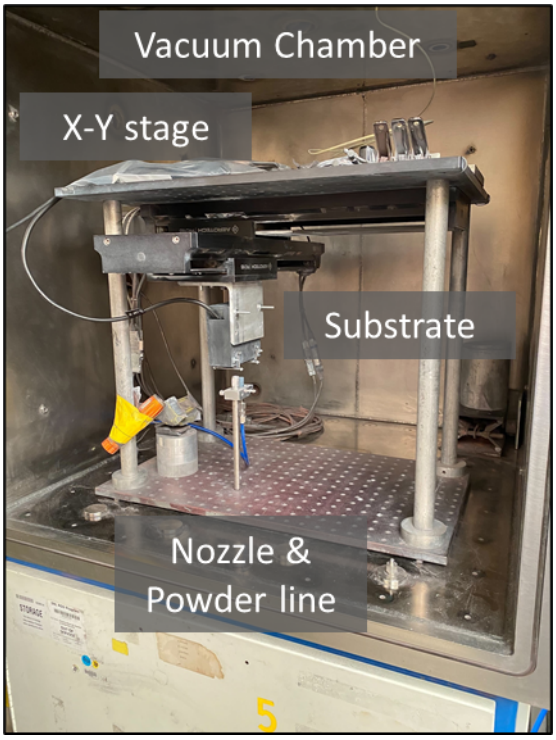

Figure A5: Labeled picture of the setup within the AD vacuum chamber.

Spray Parameters

The AD spray parameters used for all of the runs are given in Table A1.

Table A1: Aerosol deposition spray parameters.

Parameter	Value(s) or Description	Definition
Cyclone	URG Corp. 16.7LPM, 10 micron cut	Separates larger particles out of the aerosol before the powder travels through the nozzle
Carrier gas	Helium	Used to aerosolize the powder
Carrier gas flow rate (set)	84 SLPM	Flow rate of the He gas into the RBG. An Alicat is used as the He gas flow controller.
Carrier gas inlet pressure (monitored)	19 psi	Inlet pressure of the He gas into the RBG
# passes	Thin ZnO:Zn: 1 Thick ZnO:Zn: 5 ZnO:Ga: 1	Number of layers deposited
Piston packing	By hand	The RBG piston is filled with powder then packed by hand
Feed rate	10 mm/hr	Rate that the RBG piston is fed into the brush
Step size	1.2 mm	Distance between the lines of the raster pattern
Raster rate	Thin ZnO:Zn: 3600 mm/min Thick ZnO:Zn: 900 mm/min ZnO:Ga: 900 or 1800 mm/min	Rate the x-y stage is rastered over the stationary nozzle
Nozzle	Vero polymer #6, batch 1 Converging length: 18 mm Diverging length: 22 mm Inlet diameter: 4.8 mm	Converging/diverging nozzle used to accelerate the particles

	Throat diameter: 1.25 mm Outlet diameter: 1.4 mm	
Standoff	20 mm	Distance between the nozzle and the substrate
Piston diameter	14 mm	Diameter of the RBG piston
Brush saturation	After cleaning the RBG: 9 mm at 30 mm/hr then 1 mm at 10 mm/hr When RBG has not been cleaned: 4 mm at 30 mm/hr then 1 mm at 10 mm/hr	Amount of piston fed into RBG before spraying the sample

Coatings

ZnO:Zn

For the ZnO:Zn portion of the project, the goal was to produce samples for signal testing. Two ZnO:Zn coating thickness were targeted: one sample with a ZnO:Zn coating thickness of ~1 micron and a second sample with a coating as thin as possible. Both coatings were deposited on Al Almen strips.

A thick ZnO:Zn coating was successfully produced by depositing 5 passes with a raster rate of 900 mm/min (AD20231103r01). As seen in Figure A6, the coating appears homogeneous. Powder clumps were not deposited during the run. The thickness is estimated to be ~1 micron, but the roughness of the substrate makes an accurate measurement difficult.

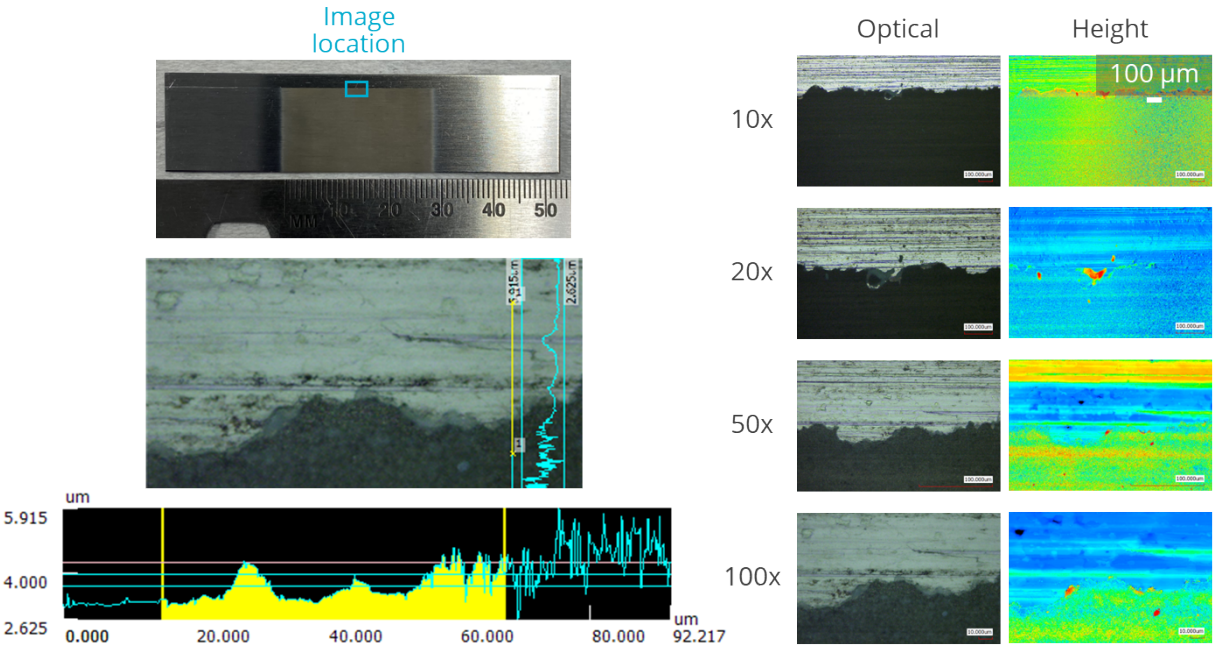

Figure A6: Keyence results for the thick ZnO:Zno coating. Optical and height images at 10x, 20x, 50x, and 100x are included along with a line height map tracing from the bare substrate onto the coating.

A thin ZnO:Zn coating was produced by depositing 1 pass with a raster rate of 3600 mm/min (AD20231103r02). The coating is difficult to see, but a faint line where the sample was masked along the top of the Almen strip can be seen in Figure A7 (similar to Figure A6). One dark spot is visible and is likely the result of a small powder clump. The coating is too thin to measure with the Keyence, but the optical images show a texture where the coating was sprayed. The sample will need to be cross sectioned and characterized using SEM to measure the coating thickness.

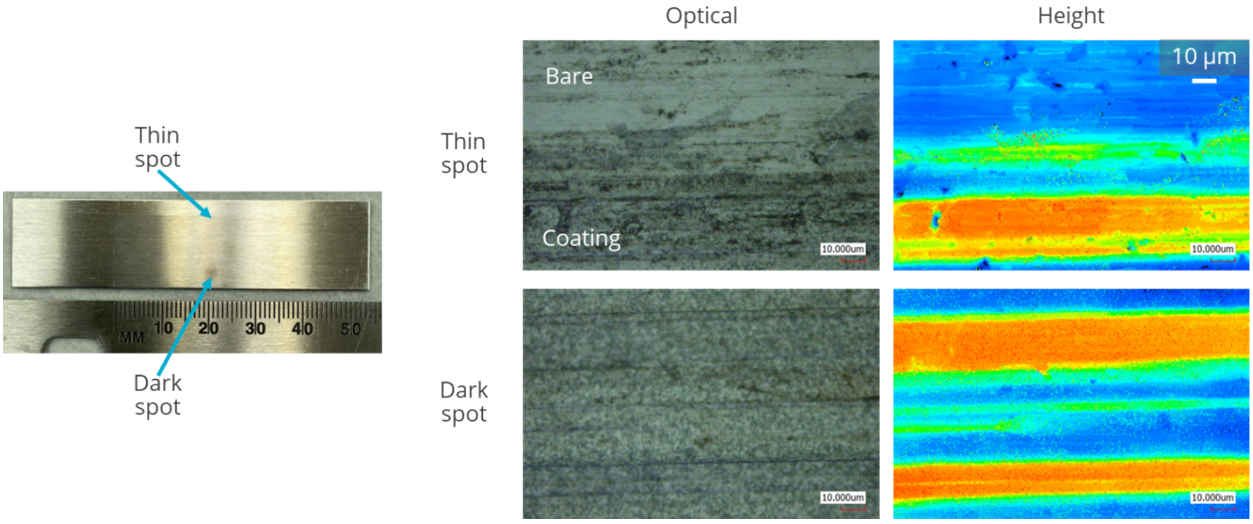

Figure A7: Keyence results for the thin ZnO:Zn coating. Based on the optical images, a coating is present, but the coating is too thin to be measured with the Keyence.

ZnO:Ga

Ball milling the ZnO powders was found to destroy the luminescent properties. So, the goal of the ZnO:Ga studies was to explore simple methods of avoiding the loss of luminescence or regaining the luminescence. One sample was sprayed using the as-received powder to avoid destroying the luminescent properties with ball milling. The second sample was sprayed using ball milled powder then heat treated in an attempt to regain the luminescence.

Two samples were sprayed during a single run using the as-received ZnO:Ga powder (AD20231218r01). One pass was deposited using a raster rate of 900 mm/min or 1800 mm/min to vary the coating thickness. Both coatings are thin but can be seen when held at an angle, as shown in Figure A8.

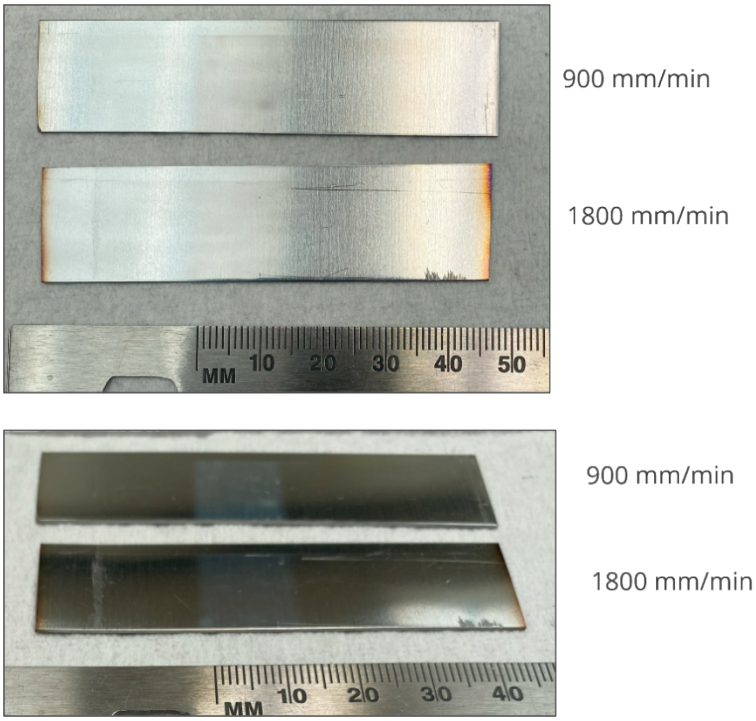

Figure A8: Pictures of the ZnO:Ga samples deposited using the as-received powder varying the raster rate.

Two more samples were sprayed during a second run using ball milled ZnO:Ga powder (AD20231218r02). Once again, a single pass was deposited using a raster rate of 900 mm/min or 1800 mm/min to vary the coating thickness. Both coatings were very splotchy and uneven. The sporadic deposition may be a result of not cleaning the cyclone before the run or powder clumping in the system. The powder is somewhat sticky which may cause some buildup in the system. It may be necessary to dry the powder and store it in a desiccator before use.

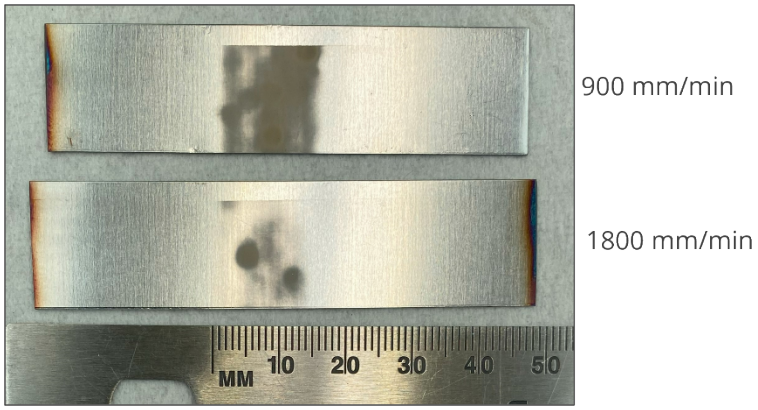

Figure A9: Picture of the ZnO:Ga samples deposited using the ball milled powder varying the raster rate.

Key takeaways:

- Ball milling ZnO:Zn and ZnO:Ga destroys their luminescent properties
- Ball milled ZnO:Zn can be deposited as a homogenous coating of various thicknesses
- As-received ZnO:Ga can be deposited as a thin layer

Next steps:

- Additional process development is needed to identify and mitigate the source of powder clumping and inhomogeneous deposition of the ball milled ZnO:Ga powder (drying the powder and storing it in a desiccator may be necessary)
- All of the thin samples should be cross sectioned and characterized using the SEM to measure the coating thickness

References

[A.1] A. Vackel, J. Therm. Spray Tech. 2020, 30(3), 584. https://doi.org/10.1007/s11666-020-01075-w

[A.2] C. A. Winters, E. M. C. Jones, J. T. Mahaffey, A. R. Jones, S. E. Murray, A. Casias, A. Grijalva, W. Flores-Brito, Developing thermophosphor digital image correlation (TP+DIC) for simultaneous strain and temperature measurements, SAND Report, SAND2021-13971, 2021